Delivery of muscle-derived exosomal miRNAs induced by HIIT improves insulin sensitivity through downregulation of hepatic FoxO1 in mice

Carlos Castaño[a,b], Mercedes Mirasierra[b,c], Mario Vallejo[b,c], Anna Novials[a,b,1], Marcelina Párrizas[a,b,1]

[a]Patogenia y Prevención de la Diabetes, Instituto de Investigaciones Biomédicas August Pi i Sunyer (IDIBAPS), Rosselló 149-153, 08036 Barcelona, Spain.
[b]Centro de Investigación Biomédica en Red de Diabetes y Enfermedades Metabólicas Asociadas (CIBERDEM), Monforte de Lemos 3-5, 28029 Madrid, Spain.
[c]Instituto de Investigaciones Biomédicas Alberto Sols, Consejo Superior de Investigaciones Científicas (CSIC) / Universidad Autónoma de Madrid (UAM), Arturo Duperier 4, 28029 Madrid, Spain

[1]Corresponding authors
Anna Novials: anovials@clinic.cat
Marcelina Párrizas: badcell@gmail.com

ORCID
Carlos Castaño: 0000-0003-1671-7826
Mercedes Mirasierra: 0000-0002-0023-8903
Mario Vallejo: 0000-0002-6422-0323
Anna Novials: 0000-0003-0465-2949
Marcelina Párrizas: 0000-0003-1296-8302

Classification: Biological Sciences
Applied Biological Sciences

Abstract

Implementation of regular physical activity helps in the maintenance of a healthy metabolic profile both in humans and mice through molecular mechanisms not yet completely defined. Here, we show that high-intensity interval training (HIIT) modifies the microRNA (miRNA) profile of circulating exosomes in mice, including significant increases in *miR-133a* and *miR-133b*. Importantly, treatment of sedentary mice with exosomes isolated from the plasma of trained mice improves glucose tolerance, insulin sensitivity and decreases plasma levels of triglycerides. Moreover, exosomes isolated from the muscle of trained mice display similar changes in miRNA content, and their administration to sedentary mice reproduces the improvement of glucose tolerance. Exosomal miRNAs upregulated by HIIT target insulin-regulated transcription factor forkhead box O1 (*FoxO1)* and, accordingly, expression of *FoxO1* is decreased in the liver of trained and exosome-treated mice. Treatment with exosomes transfected with a *miR-133b* mimic or with a specific siRNA targeting *FoxO1* recapitulates the metabolic effects observed in trained mice. Overall, our data suggests that circulating exosomes released by the muscle carry a specific miRNA signature that is modified by exercise and induce expression changes in the liver that impact whole-body metabolic profile.

Keywords

HIIT, insulin sensitivity, exosome, miRNA, *FoxO1*

Significance

The beneficial metabolic effects of exercise are mediated at least in part by the release of soluble factors by the muscles. Exosomes, small vesicles that facilitate the exchange of biological components among cells and tissues, may constitute one of these factors. Here, we show that exercise triggers the release of exosomes by the trained muscle, carrying a specific miRNA signature that induces gene expression changes in the liver, finally contributing to increased insulin sensitivity. Molecular characterization of exercise-induced exosomal miRNAs and their effects may drive the design of novel therapeutic strategies to alleviate insulin resistance and other aging-related ailments in an increasingly older society.

\body

MicroRNAs (miRNAs) are small non-coding RNA molecules that modulate gene expression in the face of physiological and pathological stresses (1). As such, they are perfectly positioned to participate in the development of diseased states (2). Importantly, aside from their canonical function, miRNAs can be released by many cells and the profile of extracellular miRNAs is modified in association with diverse pathological conditions (3). Therefore, they can be used as biomarkers to improve diagnosis and/or prognosis of metabolic diseases (4). In this regard, we have shown that the abundance of specific extracellular miRNAs is altered in prediabetic subjects and obese, glucose-intolerant mice alike (5, 6).

Extracellular miRNAs can be found bound to protein complexes, associated with high-density lipoproteins or located inside a subtype of vesicles called exosomes (7). Exosomes are released by most cell types and can be captured by other cells, where the miRNAs that they carry may induce transcriptomic changes, in essence acting as novel intercellular messengers (8). Exosomal miRNAs from cancer cells participate in tumor progression, angiogenesis and metastasis (9). Importantly, recent studies evidence that exosomal miRNAs, principally those released by the adipose tissue, regulate insulin sensitivity in other tissues (8, 10). We have recently described alterations in exosomal miRNAs in obesity, which mediate the development of metabolic disease in mice by disturbing the communication between the liver and the adipose tissue (6). Hence, if tissue crosstalk mediated by exosomal miRNAs is central to the maintenance of glucose homeostasis, they may also participate in the establishment of beneficial metabolic patterns, for instance by mediating the systemic adaptations to exercise.

The implementation of regular physical activity improves cardiorespiratory fitness (CRF) and helps maintain metabolic homeostasis (11). High CRF is a predictor of lower type 2 diabetes incidence and increased longevity (12). An array of circulating factors collectively denominated “exerkines” are secreted by the muscles during exercise and have been proposed as candidates to modulate the function of other cell types, thus improving the metabolic profile in both humans and mice (13). Interestingly, exercise also increases the number of exosomes in blood, and modifies the profile of circulating miRNAs (14, 15). These changes may contribute to the systemic signaling associated to the adaptation to exercise (16).

Recently, several studies have found that high-intensity interval training (HIIT), an exercise modality involving brief bouts of intense activity followed by periods of recovery, can elicit similar metabolic adaptations to classical endurance exercise training in humans (17). HIIT can improve CRF (18), glycemic control (19) and insulin sensitivity (17), all of them potential risk factors for the development of metabolic disease. The fact that exosomal miRNAs have been shown to respond differently as a function of the exercise modality and intensity, coupled with the lack of characterization of the underlying mechanisms of the beneficial effects of HIIT prompted us to investigate the role of exosomes in the context of the metabolic response to HIIT.

Hence, we wanted to determine if exosomal miRNAs may convey part of the beneficial effects of HIIT by modifying the function of target cells to enhance insulin sensitivity in peripheral tissues. Here, we show that HIIT triggers the release of circulating exosomes by the muscle, carrying a specific miRNA signature that induces gene expression changes in the liver, finally improving metabolic homeostasis.

Results

HIIT increases exercise capacity and improves the metabolic profile of mice. To explore the effects of exercise upon CRF and metabolism, male C57BL/6J mice were subjected to a HIIT regime for 5 weeks. As expected (20), trained mice (RUN) increased the distance traversed (Fig. 1A) and the peak oxygen uptake (Fig. 1B) during a capacity test, as compared to their sedentary control littermates (CT).

Moreover, RUN mice displayed greater glucose tolerance (Fig. 1C) demonstrated by a lower glycemia area under the curve (AUC) obtained from a glucose tolerance test (GTT) (SI Appendix Fig. S1A). RUN mice also presented lower plasma levels of triglycerides (TG) (Fig. 1D) and greater lipid tolerance (SI Appendix Fig. S1B) as measured by a TG tolerance test (TTT). Altogether, this new metabolic profile leads to greater insulin sensitivity (Fig. 1E) according to an insulin tolerance test (ITT), with a significant decrease of basal insulin levels during the GTT (SI Appendix Fig. S1C).

RUN mice also presented marginally increased circulating free-fatty acids (FFA) (Fig. 1F) which may be due to the enhanced responsiveness of the adipose tissue to lipolytic cues resulting from training (21). However, the adipose tissue of RUN mice was more sensitive to the suppressive action of insulin (22), and FFA plasma levels of RUN mice reached similar values as those of CT mice 15 min after insulin injection during the ITT (SI Appendix Fig. S1D). Accordingly, we also observed a significant decrease in body weight (SI Appendix Fig. S1E), which was mostly explained by a smaller epididymal white adipose tissue (eWAT) (SI Appendix Table S1). Overall, these findings are suggestive of improved whole-body insulin sensitivity following exercise training and, accordingly, the HOMA-IR index for the trained mice was significantly lower (SI Appendix Fig. S1F).

Circulating exosomes from RUN mice improve glucose and lipid metabolism in sedentary mice. Release of soluble factors including exosomes from skeletal muscle has been proposed to mediate the systemic adaptations to exercise (16). Hence, we isolated exosomes from equal amounts of plasma from CT and RUN mice 48h after the last exercise session. Vesicle morphology was characterized by transmission electron microscopy (Fig. 2A), size distribution was determined by nanoparticle tracking analysis (Fig. 2B) and presence of well-known exosome marker proteins was detected by western blotting (Fig. 2C). We did not observe differences in exosome number between CT and RUN mice as estimated from esterase activity levels (SI Appendix Fig. S2A).

We first studied if exogenously administered exosomes could be captured by acceptor cells by injecting control mice with PKH26-labeled exosomes intravenously (i.v.) through the tail vein. As we and others have shown before (6, 10), fluorescent signals were evident in different tissues, including liver and skeletal muscle, 6 h after the injection (Fig. 2D).

To assess the influence of exosomes upon energy metabolism, we next injected sedentary mice with exosomes isolated from plasma of either sedentary (EXO-CT) or trained mice (EXO-RUN). We found a positive correlation between total exosome protein and exosome number for both CT and RUN mice (SI Appendix Fig. S2B). Hence, i.v. injections of 15 µg exosomes, corresponding to approximately $5x10^9$ vesicles, took place biweekly during 4 weeks. Surprisingly, EXO-RUN mice showed improved glucose tolerance (Fig. 2E and SI Appendix Fig. S2C) and decreased plasma levels of TG (Fig. 2F) with improved lipid tolerance (SI Appendix Fig. S2D). However, we did not observe differences in the levels of FFA (Fig. 2G). Moreover, EXO-RUN mice were significantly leaner than their EXO-CT counterparts with smaller eWAT fat pads (SI Appendix Table S1). Finally, this treatment led to greater insulin sensitivity (Fig. 2H) as in the case of RUN mice.

Activation of fatty acid oxidation (FAO), for instance by increasing physical activity, may constitute a therapeutic target to treat insulin resistance (23). Substrate use can be assessed by measuring the respiratory exchange ratio (RER). We assessed the influence of both exercise and the exosome treatment upon energy balance through indirect calorimetry. Access to food was restricted to the night period in order to decrease the variability inside the groups. No changes were observed in either cumulative food intake (SI Appendix Fig. S2E) or total activity (SI Appendix Fig. S2F) in any group of mice. Moreover, we did not detect changes in the RER in neither the RUN nor the EXO-RUN mice (Fig. 2I) indicating unaltered substrate preference.

However, significant elevations in VO_2 uptake (Fig. 2J), CO_2 production (SI Appendix Fig. S2G) and, consequently, energy expenditure (EE) (Fig. 2K) were detected only in RUN mice, thus suggesting increases in the total rate of both FAO and carbohydrate oxidation (CHOx).

Overall, these data suggest that HIIT induces a better glycemic control by improving insulin sensitivity without changes in the RER but with a significant increase in VO_2 uptake. Importantly, the treatment with exercise-induced exosomes recapitulates the metabolic benefits without increasing EE.

HIIT modifies the miRNA content of circulating exosomes in mice. To identify the bioactive molecules responsible for the metabolic effects of exercise-induced exosomes, we focused on the miRNA content because exosomal miRNAs have been shown by us and others to participate in the establishment of metabolic phenotypes (6, 10). We isolated total RNA from plasma exosomes of RUN mice and transfected it into exosomes isolated from control mice. Hence, we generated a pool of control exosomes enriched in exercise-associated miRNAs. With this strategy, we aimed to isolate the effect of the miRNAs, discarding other sources of variation such as the protein content or lipid cover of the exosomes. As a control, we also transfected total RNA isolated from plasma exosomes of CT mice (SI Appendix Fig. S3A). Sedentary mice were then i.v. injected biweekly during 2 weeks with these transfected exosome preparations. Importantly, mice injected with control exosomes enriched with miRNAs derived from trained mice (RUNmiR) recapitulate the improvement of glucose tolerance observed in RUN and EXO-RUN mice (Fig. 3A and SI Appendix Fig. S3B). These data suggest that the exosomal miRNA content is modified by exercise and participates in the establishment of a beneficial metabolic profile.

Real time RT-PCR profiling of exosomes showed upregulation of 6 miRNAs in exosomes from RUN mice, whereas only one was significantly downregulated (Fig. 3B, S3C and SI Appendix Table S2). Interestingly, among the upregulated miRNAs we identified *miR-133a*, *miR-133b* and *miR-206*, three highly muscle-specific miRNAs (myomiRs). On the other hand, we observed downregulation of *miR-192* (SI Appendix Table S2), an exosomal miRNA that we recently described as upregulated in obesity (6). Heat map representation and principal component analysis of the most upregulated and downregulated miRNAs showed separated clustering of exosomes from CT and RUN mice (Fig. 3C and S3D). In addition, we performed a correlation analysis between each pair of miRNAs across all samples and selected those miRNAs with significant correlation to *miR-133b* ($p<0.05$). Heat map representation of those miRNAs suggests that exercise drives the release of a novel population of exosomes into the circulation (Fig. 3D).

Muscle-derived exosomes are the main contributors to the exercise-induced circulating exosomal miRNA profile. An important question is to identify which tissue is the main source of these circulating exosomes. To address this point, we isolated interstitial exosomes from liver, muscle and eWAT of CT and RUN mice by adapting a recently described strategy (24). Representative electron micrographs showed successful isolation of interstitial exosomes (Fig. 4A). We used RT-PCR to measure the expression of candidate miRNAs in these exosomes as well as the total tissues. Heat map representation showed that exosomes from muscle were enriched in *miR-133a* and *miR-133b* as compared to exosomes from liver or eWAT (Fig. 4B). Moreover, the level of these miRNAs was even higher in the case of exosomes from the muscle of RUN mice. This differential expression in exosomes followed a pattern similar to that observed in total tissues (Fig. 4C). Interestingly, we also measured the levels of 2 of the miRNAs most upregulated in obesity (6), *miR-122* and *miR-192*, both of which had a high liver expression, in both the tissue and exosomal fractions, and were decreased with exercise.

To determine which population of exosomes is involved in the observed metabolic effects, sedentary mice were injected biweekly during 4 weeks with either liver- or muscle-derived exosomes from CT and RUN mice. After the treatment, mice

injected with exosomes derived from trained muscle (Muscle exoRUN) were the only ones showing a significant effect, mimicking the improvement of glucose tolerance observed in RUN and EXO-RUN mice (Fig. 4D and E and SI Appendix Fig. S4A). The total number of interstitial exosomes is the same in CT and RUN mice for each tissue (SI Appendix Fig. S4B). Overall, these data suggest that the exosomes released by the trained muscle may be the principal agents involved in the establishment of a better response to glucose.

Treatment with exercise-induced exosomal miRNAs results in downregulation of hepatic *FoxO1*. Our data suggest that part of the beneficial effects of HIIT upon metabolism may be mediated by the upregulated exosomal miRNAs modifying the expression of target genes in peripheral tissues. Therefore, we used bioinformatics tools to identify the main pathways affected by them (SI Appendix Table S3). Network analysis provided different pathways converging on insulin-regulated transcription factor forkhead box O1 (*FoxO1)* (Fig. 5A). Notably, a comprehensive prediction of miRNA target sites using miRmap reported binding sites for most of the upregulated miRNAs in the 3' UTR of *FoxO1* (25, 26) (SI Appendix Fig. S5A). In particular, we identified 2 target sites for the *miR-133* family. There is no prior evidence of a direct regulation of *FoxO1* by *miR-133* in the literature. Hence, we transfected 3T3-L1 cells with a *miR-133b* mimic. RT-PCR analysis evidenced significant downregulation of *FoxO1* expression (SI Appendix Fig. S5B), thus suggesting that *FoxO1* is a direct target of *miR-133* family miRNAs.

Intriguingly, modulation of *FoxO1* is a potential therapy to improve insulin sensitivity (27). Hence, we analyzed *FoxO1* gene expression in both RUN and EXO-RUN mice. In the eWAT, we did not observe any changes (Fig. 5B). Moreover, Hematoxilin & Eosin staining evidenced that adipocyte size did not differ between RUN or EXO-RUN mice and their respective controls (SI Appendix Fig. S5C).

Interestingly, *FoxO1* expression remained unchanged in gastrocnemius muscle of EXO-RUN mice whereas it was significantly decreased in RUN mice (Fig. 5C). In addition, we observed an important increase in glycolytic capacity as evidenced by GPD staining at the expense of decreased oxidative capacity measured by SDH staining only in the muscle of RUN mice (SI Appendix Fig. S5D). These results are in line with previous works showing that HIIT increases the glycolytic capacity in gastrocnemius muscles (28) and induces a nearly complete slow-to fast fiber type transformation (29). Accordingly, we also observed increased membrane staining for the insulin-sensitive glucose transporter GLUT4 in muscle sections of RUN but not EXO-RUN mice (Fig. 5D). Altogether, these data suggest that HIIT improves muscle glucose uptake, but this feature is not transmitted by the treatment with exercise-induced exosomes.

Importantly, the analysis of hepatic gene expression showed downregulation of *FoxO1* (Fig. 5E) and several of its target genes (Fig. 5F) in both RUN and EXO-RUN mice. Moreover, decreased *FoxO1* expression was associated with enhanced accumulation of hepatic lipid droplets (Fig. 5G) as demonstrated by Oil Red staining and increased FFA content in both animal models (Fig. 5H). Hence, exosomes derived from exercise do not affect muscle *FoxO1* expression or its metabolic features but induce robust gene expression changes in liver.

***miR-133b* modulates hepatic gluconeogenesis both *in vitro* an *in vivo*.** Exercise is generally associated with increased glucose uptake and use by the muscles (30). In order to test if this is also the case for HIIT, we decided to measure changes in RER during a GTT in CT and RUN mice. Interestingly, RUN mice displayed significantly increased RER values during the test (Fig. 6A), indicative of a higher level of glucose oxidation. On the other hand, according to a pyruvate tolerance test (PTT), RUN mice achieve lower levels of gluconeogenesis (GNG) than CT mice (Fig. 6B), suggestive of increased hepatic insulin sensitivity. However, we did not observe changes in AKT phosphorylation in RUN mice after insulin injection (SI Appendix Fig.

S6A). This would be in accordance with the sensitizing point being downstream of AKT, as would be expected for the observed decrease in *FoxO1* expression (31).

To further explore the effects of exercise-induced exosomal miRNAs upon hepatic metabolism, we developed an *in vitro* approach (SI Appendix Fig. S6B). Primary hepatocytes were either incubated in the presence of exosomes isolated from the plasma of CT or RUN mice, or directly transfected with a *miR-133b* mimic or a siRNA against *FoxO1* as a positive control. Twenty-four hours afterwards, media were changed to serum-free medium overnight, and then the cells were challenged for 6 h with a medium containing the GNG substrates lactate and pyruvate, and the cAMP analog pCT-cAMP (32). Glucose levels measured in the media after the incubation reflect the GNG potential of the hepatocytes exposed to the different treatments. Interestingly, both the incubation with RUN exosomes and the transfection of *miR-133b* resulted in significantly decreased glucose production similar to the effects of knocking down *FoxO1* (Fig. 6C, left panel). Importantly, this effect was accompanied by significantly decreased *FoxO1* expression (Fig. 6C, right panel). Still, miR-133b and FoxO1 could be exerting their effects through parallel pathways. To provide further evidence that *mir-133b* is acting through the *FoxO1* pathway, we repeated the experiment but by overexpressing *mir-133b* in *FoxO1* knocked down hepatocytes (SI Appendix Fig. S6C). Importantly, the combination of *miR-133b* with siFoxO1 had a similar effect upon glucose production and *FoxO1* expression as each factor separately (Fig. 6D).

Overall, these data suggest that exercise-induced exosomal miRNAs decrease hepatic *FoxO1* expression, resulting in decreased GNG and improved glucose tolerance. To test this hypothesis, we transfected control exosomes with a *miR-133b* mimic and treated sedentary mice with this preparation with biweekly injections for 4 weeks. Similar to RUN mice, a PTT showed decreased GNG levels in the mice treated with the *miR-133b* mimic (Fig. 6E), and, as expected, the treatment resulted in improved glucose tolerance (Fig. 6F and SI Appendix Fig. S6D) and increased insulin sensitivity (Fig. 6G). Again, as observed for the EXO-RUN mice, no differences were detected in GLUT4 staining in muscle (SI Appendix Fig. S6E). These data further support the hypothesis that, different to the situation in the RUN mice, where improved glucose tolerance is the result of a combination of increased glucose use and decreased glucose production, the improved metabolic response in mice treated with exosomal miRNAs is mainly due to their hepatic effects.

Experimental downregulation of hepatic *FoxO1* recapitulates the effects of exosomal miRNAs upon metabolism. We hypothesized that decreased hepatic *FoxO1* expression could explain part of the phenotype of RUN and EXO-RUN mice. Hence, we used an alternative strategy by injecting sedentary mice with control exosomes transfected with siFoxO1 or a non-targeting siRNA as a control. After the treatment, we detected decreased expression of both FoxO1 (SI Appendix Fig. S7A) and its target gene *G6pc* (SI Appendix Fig. S7B) and a reduction of FOXO1 immunostaining (SI Appendix Fig. S7C) in liver. Remarkably, siFoxO1 mice presented improved glucose tolerance (Fig. 7A and SI Appendix Fig. S7D) and insulin sensitivity (Fig. 7B), with significantly decreased circulating levels of TG (Fig. 7C). Similar to RUN and EXO-RUN mice, we observed a concurrent increase in hepatic FFA (Fig. 7D) and lipid content (Fig. 7E) akin to what has been described in genetic models of *FoxO1* silencing (31, 33) which are also more insulin-sensitive than their controls. Altogether, these data show that treatment with siFoxO1-transfected exosomes decreases *FoxO1* expression in liver, and this is enough to recapitulate part of the metabolic profile of RUN mice and EXO-RUN mice (Fig. 7F).

Discussion

Our results showing improved CRF and insulin sensitivity in mice trained under a HIIT protocol are in accordance with previous evidence in humans (17–19).

Surprisingly, here we show that treatment with exosomes isolated from trained mice is able to improve glucose tolerance and insulin sensitivity in sedentary mice to a level similar to that of exercise itself.

Age and dietary excess are both characterized by insulin resistance derived from excessive fat storage due to either decreased mobilization or increased availability respectively (34). Activation of FAO, for instance by increasing physical activity, may constitute a therapeutic target to treat insulin resistance (23). However, there is controversy as to whether HIIT increases FAO. A number of studies describe significant increases in FAO, concurrent or not with increases in CHOx, in response to HIIT (35, 36) but other reports contradict these findings (37). We did not detect changes in substrate preference after HIIT. However, EE was significantly elevated in RUN mice, thus indicating increases in the total rate of both FAO and CHOx. Our treatment with exosomes from trained mice was able to recapitulate the metabolic effects of exercise but not the increase in EE. In line with these results there is controversy as to whether EE can be increased in the absence of increased physical activity (38). If this were the case, the attainment of biochemical means to mimic the effects of exercise without actually increasing physical activity would be strongly curtailed. Still, finding the pathways mediating some of the positive responses to exercise may protect patients from metabolic decline even when they are unable to exercise (38), an important objective in a progressively ageing society.

Different reports have demonstrated that exercise induces the release of exosomes enriched in specific miRNAs following different time-courses depending on the exercise type (39). Although some studies have shown increased exosome number with exercise (39), we did not observe this effect. This discrepancy may be due to either the exercise modality or the timing of sample collection. Our data show that the circulating exosome pool in trained mice is significantly enriched in vesicles released by the skeletal muscle, in agreement with previous reports (40). In particular, we observed upregulation of *miR-133a*, *miR-133b* and *miR-206*, three myomiRs whose circulating levels in vesicles have been shown by others to be increased in correlation with VO_2 max in humans (41). Moreover, several of these miRNAs have already been linked with improved insulin sensitivity in different animal models (25, 26).

We identified binding sites for most of the upregulated miRNAs in the 3' UTR of *FoxO1.* Conditional *FoxO1* ablation in skeletal muscle results in increased formation of MyoD-containing fast fibers and altered fiber type distribution at the expense of myogenin-containing slow fibers (42). Decreased expression of FoxO1 in the gastrocnemius muscle after HIIT has already been shown in rats (43). Remarkably, we detected muscle *FoxO1* downregulation only in trained mice, which may indicate that this adaptation is dependent on the direct effect of exercise and not mediated by exosomal miRNAs. Conversely, lack of effect of the exogenous exosomes upon muscle *FoxO1* expression could be due to the specific route of administration. However, exogenous PKH26-labeled exosomes reach the muscle. Additionally, in a previous experiment we injected exosomes transfected with nonmammalian miRNA, *cel-miR-39-3p* (6), and were able to detect its presence by real time RT-PCR in muscle (Ct 30.5 ± 0.1), liver (Ct 26.7 ± 0.2) and eWAT (Ct 34.3 ± 2.9). Overall, these data would argue that the exosomes, albeit with a preference for the liver, reach the muscle, but the exercise-induced miRNAs do not affect the expression of, at least, our identified target *FoxO1*. It is important to note that, in contrast to the pharmacological-like effects of siRNAs, the effects of miRNAs are largely context dependent (44), and the *miR-133* family is expressed at high levels in the muscle, while being almost absent in liver (see Fig. 4C). Hence, it is not surprising that we observe a higher effect in the latter tissue. In addition, we detected other changes in the muscle of RUN mice that are not mirrored in the EXO-RUN mice, such as increased GLUT4 expression and GPD activity. We postulate that these changes, as well as the enhanced EE of RUN mice, are independent of the exercise-induced exosomal miRNAs and dependent on exercise itself.

Exercise-derived exosomes have been shown to display liver tropism when i.v. administered (45). Accordingly, we observed downregulation of hepatic *FoxO1* and several of its target genes in both RUN and EXO-RUN mice. Hepatic glucose production is finely controlled by insulin signaling that dampens *FoxO1* and reins in gluconeogenesis (46), although at the expense of increased *de novo* lipogenesis leading to hepatic lipid storage (33). This same phenotype of enhanced insulin sensitivity and hepatic fat accumulation is reproduced in mice injected with exosomes transfected with siFoxO1, in accordance with previous reports showing that *FoxO1* knock-down is a possible therapeutic strategy for improving insulin resistance (47). However due its bivalent effects, alternative approaches, such as selective inhibition of specific *FoxO1* target genes have been proposed to lower glycemia without concurrent steatosis (48).

Altogether, our data indicate that HIIT improves glucose tolerance both by increasing glucose use, as measured by the higher RER values during a GTT, and by decreasing endogenous glucose production, as evidenced by a PTT. In this sense, HIIT has been recently shown to improve hepatic insulin sensitivity and decrease endogenous glucose production in insulin resistant humans (49). For this reason, HIIT is becoming the preferred exercise modality to improve glucose levels in prediabetic patients with impaired fasting glucose, which are mainly characterized by reduced hepatic insulin sensitivity (50–52). Importantly, treatment with exercise-induced exosomes or direct transfection of *miR-133b* decrease *FoxO1* expression and hepatocyte glucose production *in vitro*. Moreover, transfection of *miR-133b* in *FoxO1* knocked down hepatocytes did not further decrease glucose production than *FoxO1* knockdown alone. This, together with the fact that *miR-133b* is able to decrease *FoxO1* expression in 3T3-L1 cells and in primary hepatocytes suggest that the miRNA is exerting at least part of its effects through *FoxO1*. However we cannot discard that additional *miR-133b* targets are also weighing in, as miRNAs regulate a wide range of genes. Finally, mice treated with *miR-133b* transfected exosomes also show improved glucose tolerance associated with decreased GNG.

Overall, we show that HIIT triggers the release of circulating exosomes by the trained muscle, carrying a specific miRNA signature that induces gene expression changes in the liver, leading to an improved metabolic profile. Our data suggest that exosomes from athletes or control exosomes bioengineered to incorporate specific miRNAs or short interfering RNAs (siRNAs) may be useful in the treatment of metabolic disorders (38).

Materials and Methods

Experimental animal models. C57BL/6J Male mice were used in all experiments. RUN: mice were subjected to a HIIT protocol for 5 weeks (53). EXO-RUN: mice were injected i.v. through the tail vein with a 100 μl PBS suspension containing 15 μg exosomes isolated from plasma of either sedentary or trained mice. EXOmiR: mice were injected with 25 μg exosomes isolated from plasma of control mice and transfected with total RNA isolated from 7 μg of either sedentary or trained plasma exosomes. iEXO: mice were injected with 7 μg interstitial exosomes isolated from liver or muscle of either sedentary or trained mice. miR-133b: mice were injected with 25 μg exosomes transfected with 125 pmol *miR-133b* mimic. siFoxO1: mice were injected with 25 μg exosomes transfected with 190 pmol of siFoxO1 or a non-targeting siRNA. Biodistribution studies: mice were injected with 100 μg exosomes labeled with the fluorescent dye PKH26 and sacrificed 6 h afterwards. Metabolic tests were performed as described (6). Indirect calorimetry, was carried out using a 16-chamber TSE PhenoMaster monitoring system (54). Studies were conducted in accordance with principles of laboratory animal care (register: 46/18).

Exosome characterization. Exosomes were isolated from mouse plasma as described (6). Interstitial exosomes were isolated by adapting a recently described

protocol (24). Exosome transfections were performed with the Exo-Fect Exosome Transfection Reagent as described (6) using the miRNA mimics and siRNAs described in SI Appendix Table S4.

Cell culture and *in vitro* experiments. 3T3-L1 cells and primary hepatocytes were transfected with 60 nM siFoxO1 and 30 nM *miR-133b-3p* either in parallel in separate wells or sequentially in the same well (SI Appendix Table S4) by using Metafectene Pro (6). Primary hepatocytes were incubated with 7 μg/ml exosomes isolated from CT or RUN mice. Hepatocyte glucose production was determined by measuring glucose concentration in the media as described (32).

RNA analysis. RNA was extracted from 10 μl plasma exosomes or 30 μl interstitial exosomes with miRNeasy Mini Kit and retrotranscribed with mircury LNA Universal RT Kit. Profiling of 378 miRNAs was performed by Real time RT-PCR. For tissue samples, RNA was extracted with TRIreagent and analyzed by RT-PCR using the High-Capacity RT Kit and homemade primers (SI Appendix Table S4).

Protein analysis. Protein lysates were resolved by SDS-PAGE and visualized by blotting with HRP-conjugated secondary antibodies. For histochemistry, liver and muscle were frozen in liquid N_2-cooled isopentane and embedded in OCT. eWAT was fixed with 4% PFA and embedded in paraffin. Hematoxylin & Eosin and Oil Red staining were performed by following the protocols at IHCWorld. Gastrocnemius sections were stained as described (55). For GLUT4 immunohistochemistry, muscle cryostat sections were stained with 1:100 anti-GLUT4 (1F8) antibody. For FOXO1 immunohistochemistry, liver sections were stained with 1:100 FoxO1 (C29H4) antibody.

Statistical analyses. Differences between groups were determined by either t-test analysis when only two groups were compared or by One-way ANOVA with t-test analysis for the pair wise comparison of 3 or more groups with different number of values. Asterisks indicate significance with respect to control group, unless otherwise specified. Correlation analyses were performed by Pearson regression.

ACKNOWLEDGMENTS

We thank the members of the Electron Microscopy Unit from the CCiTUB. We thank H.A. del Portillo from ISGlobal and IGTP for his help in the NTA analyses. We thank P.M. García-Roves from IDIBELL for critical discussion of the results. We thank M. Batlle from IDIBAPS for help with calorimetry studies. This work was supported by Grant EFSD/Lilly-2013, Menarini, CIBERDEM, Fundació l'Acadèmia, Project 2017_SGR of the DURSI (A.N.), and grant BFU2017-89336-R from Spanish MINECO (M.V.). The authors declare no conflict of interest.

AUTHOR CONTRIBUTIONS

C.C., M.P. and A.N. designed research; C.C. and M.P. performed research; C.C., M.M., M.V. analyzed data; C.C., M.P. and A.N. wrote the paper.

REFERENCES

1. Bartel DP (2009) MicroRNAs: target recognition and regulatory functions. *Cell* 136(2):215–233.
2. Mendell JT, Olson EN (2012) MicroRNAs in stress signaling and human disease. *Cell* 148(6):1172–87.
3. Mori MA, Ludwig RG, Garcia-Martin R, Brandao BB, Kahn CR (2019) Extracellular miRNAs: From Biomarkers to Mediators of Physiology and Disease. *Cell Metab* 30(4):656–673.
4. Parrizas M, Novials A, Párrizas M, Novials A (2016) Circulating microRNAs as biomarkers for metabolic disease. *Best Pract Res Clin Endocrinol Metab* 30(5):591–601.

5. Párrizas M, et al. (2015) Circulating miR-192 and miR-193b are markers of prediabetes and are modulated by an exercise intervention. *J Clin Endocrinol Metab* 100(3):E407–E415.

6. Castaño C, Kalko S, Novials A, Párrizas M (2018) Obesity-associated exosomal miRNAs modulate glucose and lipid metabolism in mice. *Proc Natl Acad Sci USA* 115(48):12158–12163.

7. Castaño C, Novials A, Párrizas M (2019) Exosomes and diabetes. *Diabetes Metab Res Rev* 2019:e3107.

8. Thomou T, et al. (2017) Adipose-derived circulating miRNAs regulate gene expression in other tissues. *Nature* 542(7642):450–455.

9. Fong MY, et al. (2015) Breast-cancer-secreted miR-122 reprograms glucose metabolism in premetastatic niche to promote metastasis. *Nat Cell Biol* 17(2):183–194.

10. Ying W, et al. (2017) Adipose Tissue Macrophage-Derived Exosomal miRNAs Can Modulate In Vivo and In Vitro Insulin Sensitivity. *Cell* 171(2):372-384.

11. Lin X, et al. (2015) Effects of Exercise Training on Cardiorespiratory Fitness and Biomarkers of Cardiometabolic Health: A Systematic Review and Meta-Analysis of Randomized Controlled Trials. *J Am Heart Assoc* 4(7):e002014.

12. Zaccardi F, et al. (2015) Cardiorespiratory fitness and risk of type 2 diabetes mellitus: A 23-year cohort study and a meta-analysis of prospective studies. *Atherosclerosis* 243(1):131–137.

13. Karstoft K, Pedersen BK (2016) Skeletal muscle as a gene regulatory endocrine organ. *Curr Opin Clin Nutr Metab Care* 19(4):270–275.

14. Frühbeis C, Helmig S, Tug S, Simon P, Krämer-Albers EM (2015) Physical exercise induces rapid release of small extracellular vesicles into the circulation. *J Extracell Vesicles* 4:28239.

15. Baggish AL, et al. (2011) Dynamic regulation of circulating microRNA during acute exhaustive exercise and sustained aerobic exercise training. *J Physiol* 589(16):3983–3994.

16. Safdar A, Saleem A, Tarnopolsky MA (2016) The potential of endurance exercise-derived exosomes to treat metabolic diseases. *Nat Rev Endocrinol* 12(9):504–517.

17. Gallo-Villegas J, et al. (2018) Efficacy of high-intensity, low-volume interval training compared to continuous aerobic training on insulin resistance, skeletal muscle structure and function in adults with metabolic syndrome: study protocol for a randomized controlled clinical trial. *Trials* 19(1):144.

18. Gerosa-Neto J, et al. (2019) High- or moderate-intensity training promotes change in cardiorespiratory fitness, but not visceral fat, in obese men: A randomised trial of equal energy expenditure exercise. *Respir Physiol Neurobiol* 266:150–155.

19. Metcalfe RS, et al. (2018) Extremely short duration interval exercise improves 24-h glycaemia in men with type 2 diabetes. *Eur J Appl Physiol* 118(12):2551–2562.

20. Menz V, et al. (2019) Functional Vs. Running Low-Volume High-Intensity Interval Training: Effects on VO2max and Muscular Endurance. *J Sports Sci Med* 18(3):497–504.

21. Glisezinski I de, et al. (1998) Endurance training changes in lipolytic

responsiveness of obese adipose tissue. *Am J Physiol Metab* 275(6):E951–E956.

22. Polak J, et al. (2005) Dynamic strength training improves insulin sensitivity and functional balance between adrenergic alpha 2A and beta pathways in subcutaneous adipose tissue of obese subjects. *Diabetologia* 48(12):2631–2640.

23. Clapham JC, Storlien LH (2006) The fatty acid oxidation pathway as a therapeutic target for insulin resistance. *Expert Opin Ther Targets* 10(5):749–757.

24. Crewe C, et al. (2018) An Endothelial-to-Adipocyte Extracellular Vesicle Axis Governed by Metabolic State. *Cell* 175:695–708.

25. Langlet F, et al. (2018) microRNA-205-5p is a modulator of insulin sensitivity that inhibits FOXO function. *Mol Metab* 17:49–60.

26. Wu H, et al. (2017) MicroRNA-206 prevents hepatosteatosis and hyperglycemia by facilitating insulin signaling and impairing lipogenesis. *J Hepatol* 66(4):816–824.

27. Kousteni S (2012) FoxO1, the transcriptional chief of staff of energy metabolism. *Bone* 50(2):437–443.

28. Abe T, et al. (2015) High-intensity interval training-induced metabolic adaptation coupled with an increase in Hif-1α and glycolytic protein expression. *J Appl Physiol* 119(11):1297–1302.

29. Eigendorf J, et al. (2018) High Intensity High Volume Interval Training Improves Endurance Performance and Induces a Nearly Complete Slow-to-Fast Fiber Transformation on the mRNA Level. *Front Physiol* 9:601.

30. Stanford KI, Goodyear LJ (2014) Exercise and type 2 diabetes: molecular mechanisms regulating glucose uptake in skeletal muscle. *Adv Physiol Educ* 38(4):308–314.

31. Lu M, et al. (2012) Insulin regulates liver metabolism in vivo in the absence of hepatic Akt and Foxo1. *Nat Med* 18(3):388–395.

32. Matsumoto M, Pocai A, Rossetti L, Depinho RA, Accili D (2007) Impaired regulation of hepatic glucose production in mice lacking the forkhead transcription factor Foxo1 in liver. *Cell Metab* 6(3):208–216.

33. Haeusler RA, et al. (2014) Integrated control of hepatic lipogenesis versus glucose production requires FoxO transcription factors. *Nat Commun* 5:5190.

34. Anton SD, et al. (2018) Flipping the Metabolic Switch: Understanding and Applying the Health Benefits of Fasting. *Obesity* 26(2):254–268.

35. Talanian JL, Galloway SDR, Heigenhauser GJF, Bonen A, Spriet LL (2007) Two weeks of high-intensity aerobic interval training increases the capacity for fat oxidation during exercise in women. *J Appl Physiol* 102(4):1439–1447.

36. Perry CGR, Heigenhauser GJF, Bonen A, Spriet LL (2008) High-intensity aerobic interval training increases fat and carbohydrate metabolic capacities in human skeletal muscle. *Appl Physiol Nutr Metab* 33(6):1112–1123.

37. Astorino TA, et al. (2017) Change in maximal fat oxidation in response to different regimes of periodized high-intensity interval training (HIIT). *Eur J Appl Physiol* 117(4):745–755.

38. Booth FW, Laye MJ (2009) Lack of adequate appreciation of physical exercise's complexities can pre-empt appropriate design and interpretation in scientific

discovery. *J Physiol* 587(Pt 23):5527–5539.

39. Wilhelm EN, Mourot L, Rakobowchuk M (2018) Exercise-Derived Microvesicles: A Review of the Literature. *Sports Med* 48(9):2025–2039.

40. Nielsen S, et al. (2010) Muscle specific microRNAs are regulated by endurance exercise in human skeletal muscle. *J Physiol* 588(20):4029–4037.

41. Guescini M, et al. (2015) Muscle Releases Alpha-Sarcoglycan Positive Extracellular Vesicles Carrying miRNAs in the Bloodstream. *PLoS One* 10(5):e0125094.

42. Kitamura T, et al. (2007) A Foxo/Notch pathway controls myogenic differentiation and fiber type specification. *J Clin Invest* 117(9):2477–2485.

43. Biglari S, Afousi AG, Mafi F, Shabkhiz F (2020) High-intensity interval training-induced hypertrophy in gastrocnemius muscle via improved IGF-I/Akt/FoxO and myostatin/Smad signaling pathways in rats. *Physiol Int*. doi:10.1556/2060.2020.00020.

44. Erhard F, et al. (2014) Widespread context dependency of microRNA-mediated regulation. *Genome Res* 24(6):906–919.

45. Whitham M, et al. (2018) Extracellular Vesicles Provide a Means for Tissue Crosstalk during Exercise. *Cell Metab* 27(1):237–251.

46. Cheng Z (2015) FoxO1: mute for a tuned metabolism? *Trends Endocrinol Metab* 26(8):402–403.

47. Samuel VT, et al. (2006) Targeting Foxo1 in mice using antisense oligonucleotide improves hepatic and peripheral insulin action. *Diabetes* 55(7):2042–2050.

48. Langlet F, et al. (2017) Selective Inhibition of FOXO1 Activator/Repressor Balance Modulates Hepatic Glucose Handling. *Cell* 171(4):824-835.

49. Apostolopoulou M, et al. (2018) Effects on Insulin Sensitivity, but Not on Mitochondrial Function Are Dependent on Insulin Resistance Status after High Intensity Interval Training. *Diabetes* 67(Supl.1):69-OR.

50. Marquis-Gravel G, et al. (2015) Intensive lifestyle intervention including high-intensity interval training program improves insulin resistance and fasting plasma glucose in obese patients. *Prev Med reports* 2:314–318.

51. Weber MB, et al. (2016) The Stepwise Approach to Diabetes Prevention: Results From the D-CLIP Randomized Controlled Trial. *Diabetes Care* 39(10):1760–1767.

52. Faerch K, Borch-Johnsen K, Holst JJ, Vaag A (2009) Pathophysiology and aetiology of impaired fasting glycaemia and impaired glucose tolerance: does it matter for prevention and treatment of type 2 diabetes? *Diabetologia* 52(9):1714–1723.

53. Marcinko K, et al. (2015) High intensity interval training improves liver and adipose tissue insulin sensitivity. *Mol Metab* 4(12):903–915.

54. Molinero A, et al. (2017) Muscle IL-6 in gender-specific metabolism. *PLoS One* 12:e0173675.

55. Garcia-Roves PM, Osler ME, Holmstrom MH, Zierath JR (2008) Gain-of-function R225Q mutation in AMP-activated protein kinase gamma3 subunit increases mitochondrial biogenesis in glycolytic skeletal muscle. *J Biol Chem* 283(51):35724–35734.

FIGURE LEGENDS

Fig. 1. HIIT increases exercise capacity and improves the metabolic profile of mice. (A-B) Distance run (A) and peak oxygen uptake (B) of sedentary mice (CT) and mice trained under a HIIT regime for 5 weeks (RUN) during a capacity test. (C-F) GTT (C), plasma TG (D), ITT (E) and FFA concentration (F) of the same mice at the end of the training period. Data are presented as mean ± SEM. n=4 (A, B); n=6 (C, E); n=19 CT and n=24 RUN (D); n=11 CT and n=14 RUN (F) *p<0.05, **p<0.01, ****p<0.001, Student's t-test.

Fig. 2. Circulating exosomes from RUN mice improve glucose and lipid metabolism in sedentary mice. (A-C) Representative electron micrograph (A), size distribution determined by NTA (B) and western blots of CD63, CD9 and HSP90 (C) of exosomes isolated from plasma of CT and RUN mice. (D) Liver (upper) and muscle (lower) sections of control mice 6 h after i.v. injection with PBS (left) or PKH26-labeled exosomes (right). (E-H) GTT of sedentary mice after 4 weeks of biweekly injections with exosomes isolated from either CT (EXO-CT) or RUN (EXO-RUN) mice plasma (E), plasma TG (F), FFA concentration (G) and ITT (H) in the same mice. (I-K) RER (I), VO_2 uptake (J) and EE (K) of CT, RUN and EXO-RUN mice obtained by indirect calorimetry. Data are presented as mean ± SEM. n=2 (A, B, C, D); n=5 (E, H); n=12 (F, G); n=4 (I, J, K); *p<0.05, ****p<0.001 with respect to their respective control groups, Student's t-test.

Fig. 3. HIIT modifies the miRNA content of circulating exosomes in mice. (A) GTT in sedentary mice after 2 weeks of injections of exosomes transfected with miRNAs isolated from plasma exosomes of CT (CTmiR) or RUN mice (RUNmiR). (B) Volcano plot of real time RT-PCR profiling of the miRNA content of plasma exosomes of CT and RUN mice. (C) Heat map showing clustering of exosomes from CT and RUN mice according to the most up- and downregulated miRNAs in exosomes of RUN mice. (D) Heat map showing miRNAs with significant positive (red) or negative (green) correlations to *miR-133b*. Data are presented as mean ± SEM. n=3 (A); n=4 (B, C, D); *p<0.05, Student's t-test.

Fig. 4. Muscle-derived exosomes are the main contributors to the exercise-induced circulating exosomal miRNA profile. (A) Electron micrographs of exosomes isolated from eWAT, liver and muscle from RUN mice. Arrows indicate representative exosomes. (B-C) Heat maps showing differential expression of selected miRNAs amongst exosomes isolated from muscle, liver and eWAT (B) or the total tissues (C) from CT and RUN mice. (D-E) GTT in sedentary mice after 4 weeks of injections of liver-derived exosomes (Liver exoCT and Liver exoRUN) (D) and muscle-derived exosomes (Liver exoRUN and Muscle exoRUN) from the same mice (E). Data are presented as mean ± SEM. n=2 (A); n=6 (B); n=4 (C); n=3 (D, E); *p<0.05 with respect to their respective control groups, Student's t-test.

Fig. 5. Treatment with exercise-induced exosomal miRNAs results in downregulation of hepatic *FoxO1*. (A) Network showing the interaction of some of the candidate target genes of exosomal miRNAs upregulated after HIIT. (B-C) *FoxO1* expression in the eWAT (B) and gastrocnemius (C) of CT, RUN, EXO-CT and EXO-RUN mice. (D) Representative immunostaining of GLUT4 (green) in muscle sections of the same mice. (E-F) Expression of *FoxO1* (E) and a selection of its targets in the liver of the same mice (F). (G-H) Representative Oil Red staining (G) and FFA content in liver of the same mice (H). Data are presented as mean ± SEM. n=4 in RUN model and n=6 in EXO model (B, C); n=4 (D, G); n=8 (E, F); n=16 in RUN model and n=6 in EXO model (H); *p<0.05, **p<0.01, ***p<0.005 with respect to their respective control groups, Student's t-test.

Fig. 6. *miR-133b* modulates hepatic GNG both *in vitro* an *in vivo*. (A-B) RER values during a GTT (A) and PTT (B) performed in CT and RUN mice. (C) Glucose production and *FoxO1* expression in primary hepatocytes transfected with a nontargeting siRNA (siC), a siRNA against *FoxO1* (siFoxO1), a *miR-133b* mimic (miR-133b) or incubated with exosomes isolated from plasma of CT and RUN mice (EXO-CT and EXO-RUN). (D) Glucose production and *FoxO1* expression in primary hepatocytes transfected with siC or siFoxO1, and subsequently with a *cel-miR-39-3p* mimic as a negative control or miR-133b. (E-G) PTT (E), GTT (F) and ITT (G) in sedentary mice after 4 weeks of injections of control exosomes loaded with negative control *cel-miR-39-3p* or *miR-133b* mimic. Data are presented as mean ± SEM. n=6 (A, B); n=5 (C, E, F, G); n=3 (D); *p<0.05, **p<0.01, ***p<0.005 , ****p<0.001, Student's t-test.

Fig. 7. Experimental downregulation of hepatic FoxO1 recapitulates the effects of exosomal miRNAs upon metabolism. (A-C) GTT (A), ITT (B) and plasma TG (C) in sedentary mice after 4 weeks of injections of control exosomes loaded with a nontargeting siRNA (siC) or a siRNA against FoxO1 (siFoxO1). (D-E) Representative Oil Red staining (D) and FFA content (E) in liver of the same mice. (F) Proposed model. Data are presented as mean ± SEM. n=5 (A, C, E); n=4 (B, D); *p<0.05, **p<0.01, ****p<0.001, Student's t-test.

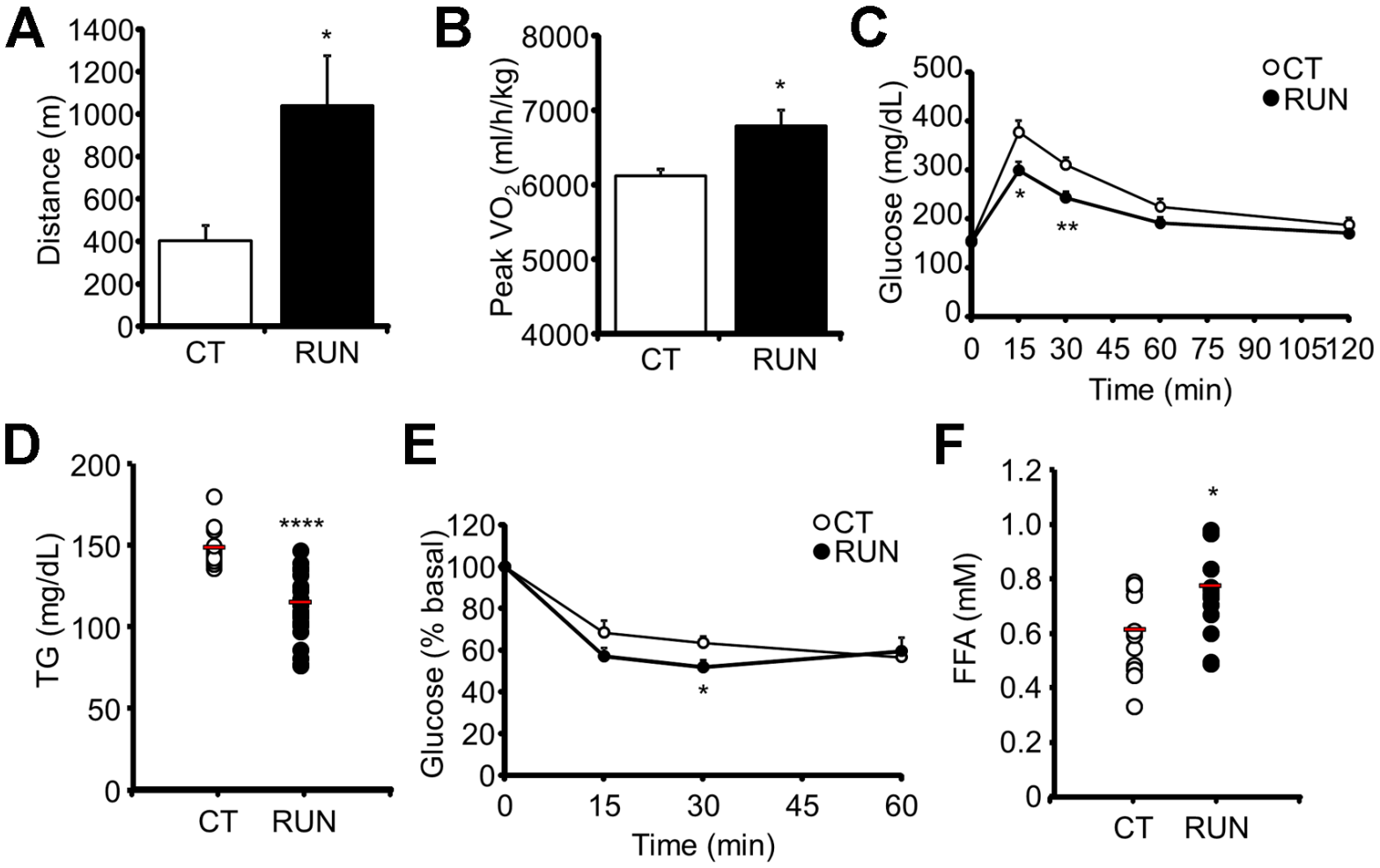
A
Distance (m)
1400
1200
1000
800
600
400
200
0
*
CT
RUN
B
Peak VO2 (ml/h/kg)
8000
7000
6000
5000
4000
*
CT
RUN
C
Glucose (mg/dL)
500
400
300
200
100
0
CT
RUN
*
**
0 15 30 45 60 75 90 105 120
Time (min)
D
TG (mg/dL)
200
150
100
50
0
****
CT
RUN
E
Glucose (% basal)
120
100
80
60
40
20
0
CT
RUN
*
0 15 30 45 60
Time (min)
F
FFA (mM)
1.2
1.0
0.8
0.6
0.4
0.2
0
*
CT
RUN

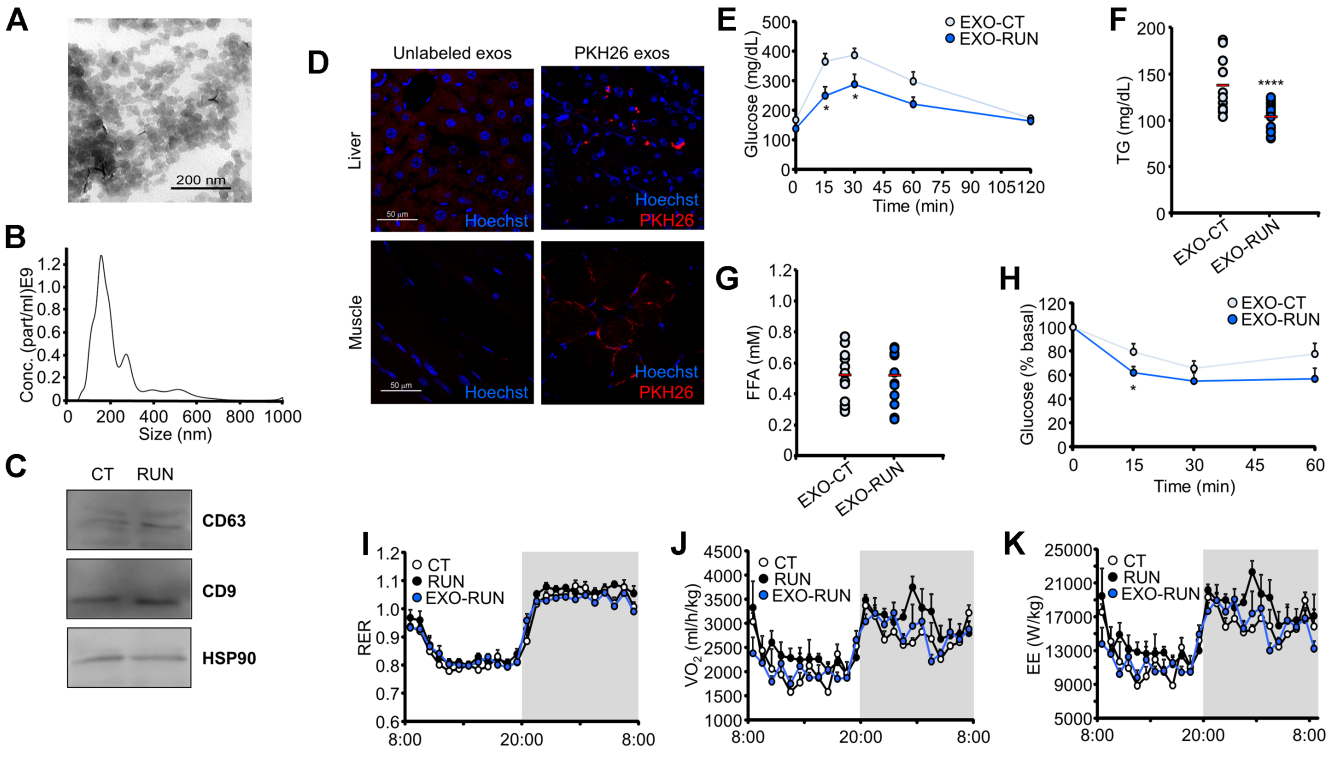
A
200 nm
B
Conc. (part/ml)E9
Size (nm)
C
CT
RUN
CD63
CD9
HSP90
D
Unlabeled exos
PKH26 exos
Liver
Muscle
Hoechst
PKH26
E
EXO-CT
EXO-RUN
Glucose (mg/dL)
Time (min)
F
TG (mg/dL)
****
G
FFA (mM)
H
Glucose (% basal)
I
RER
J
VO2 (ml/h/kg)
K
EE (W/kg)
CT
RUN
EXO-RUN
8:00
20:00

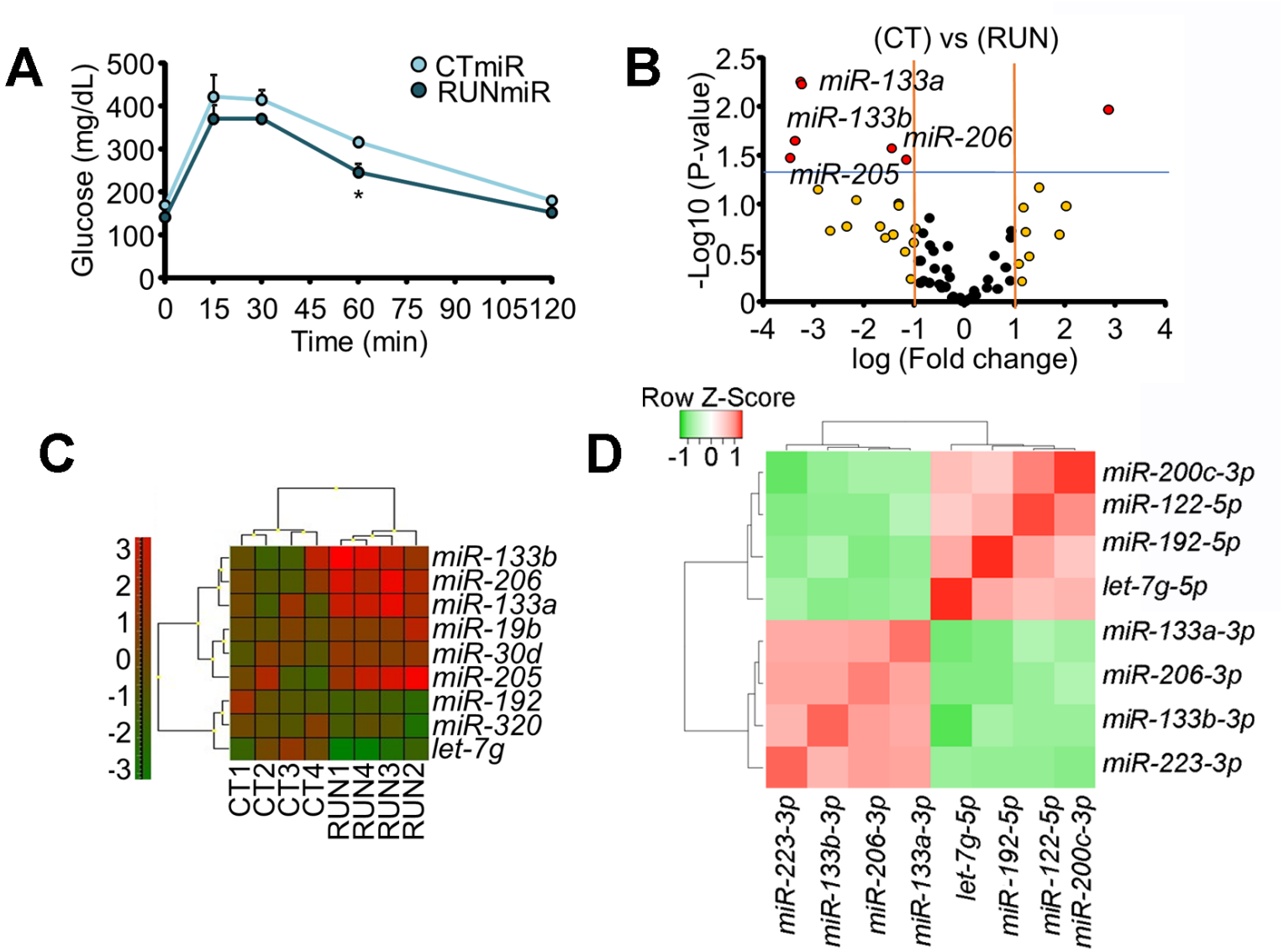
A
Glucose (mg/dL)
500
400
300
200
100
0
CTmiR
RUNmiR
*
0 15 30 45 60 75 90 105120
Time (min)
B
(CT) vs (RUN)
-Log10 (P-value)
2.5
2.0
1.5
1.0
0.5
0
miR-133a
miR-133b
miR-206
miR-205
-4 -3 -2 -1 0 1 2 3 4
log (Fold change)
C
3
2
1
0
-1
-2
-3
miR-133b
miR-206
miR-133a
miR-19b
miR-30d
miR-205
miR-192
miR-320
let-7g
CT1
CT2
CT3
CT4
RUN1
RUN4
RUN3
RUN2
D
Row Z-Score
-1 0 1
miR-200c-3p
miR-122-5p
miR-192-5p
let-7g-5p
miR-133a-3p
miR-206-3p
miR-133b-3p
miR-223-3p
miR-223-3p
miR-133b-3p
miR-206-3p
miR-133a-3p
let-7g-5p
miR-192-5p
miR-122-5p
miR-200c-3p

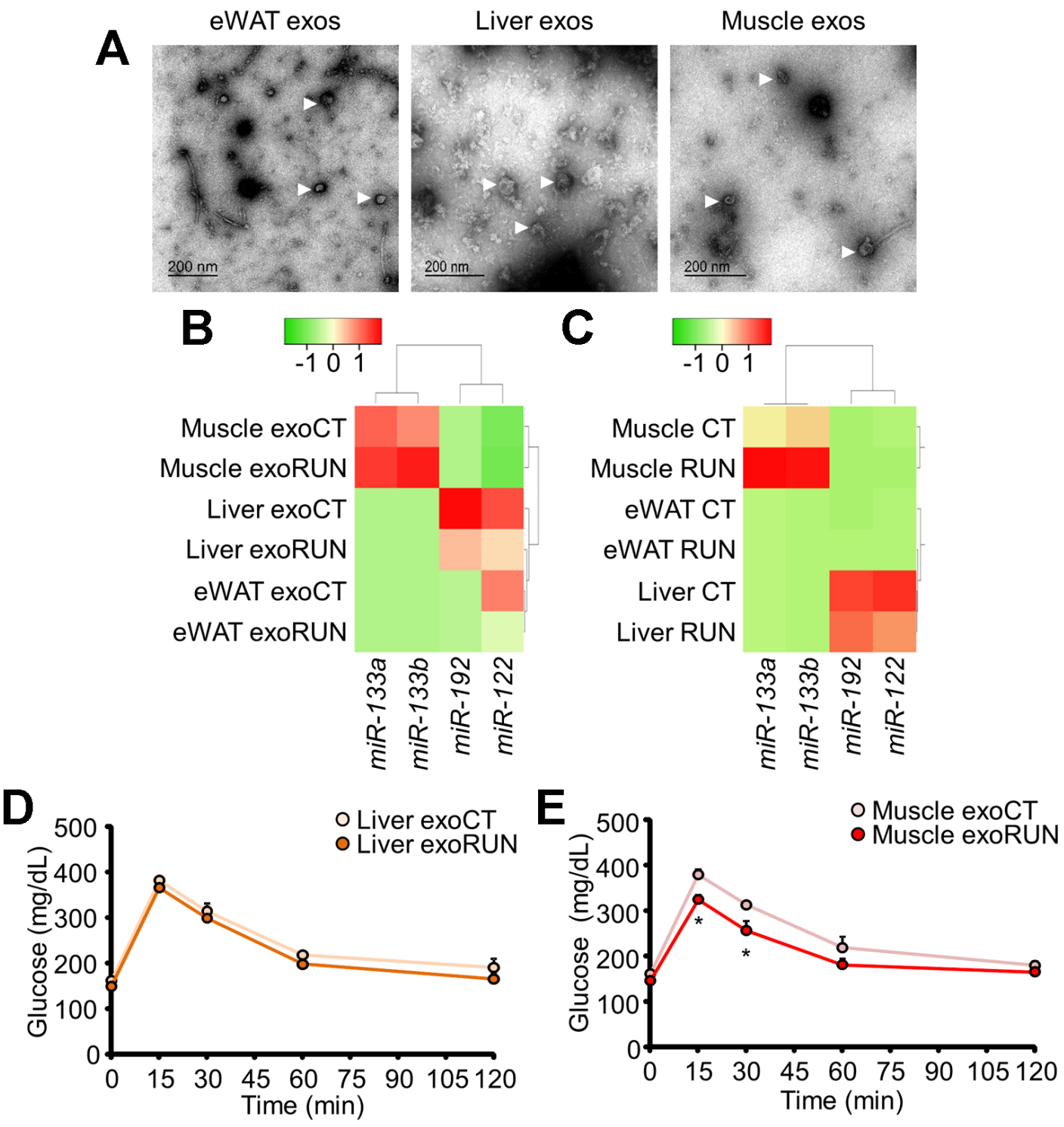
A
eWAT exos
Liver exos
Muscle exos
200 nm
200 nm
200 nm
B
-1 0 1
Muscle exoCT
Muscle exoRUN
Liver exoCT
Liver exoRUN
eWAT exoCT
eWAT exoRUN
miR-133a
miR-133b
miR-192
miR-122
C
-1 0 1
Muscle CT
Muscle RUN
eWAT CT
eWAT RUN
Liver CT
Liver RUN
miR-133a
miR-133b
miR-192
miR-122
D
Liver exoCT
Liver exoRUN
Glucose (mg/dL)
0
100
200
300
400
500
0 15 30 45 60 75 90 105 120
Time (min)
E
Muscle exoCT
Muscle exoRUN
Glucose (mg/dL)
0
100
200
300
400
500
*
*
0 15 30 45 60 75 90 105 120
Time (min)

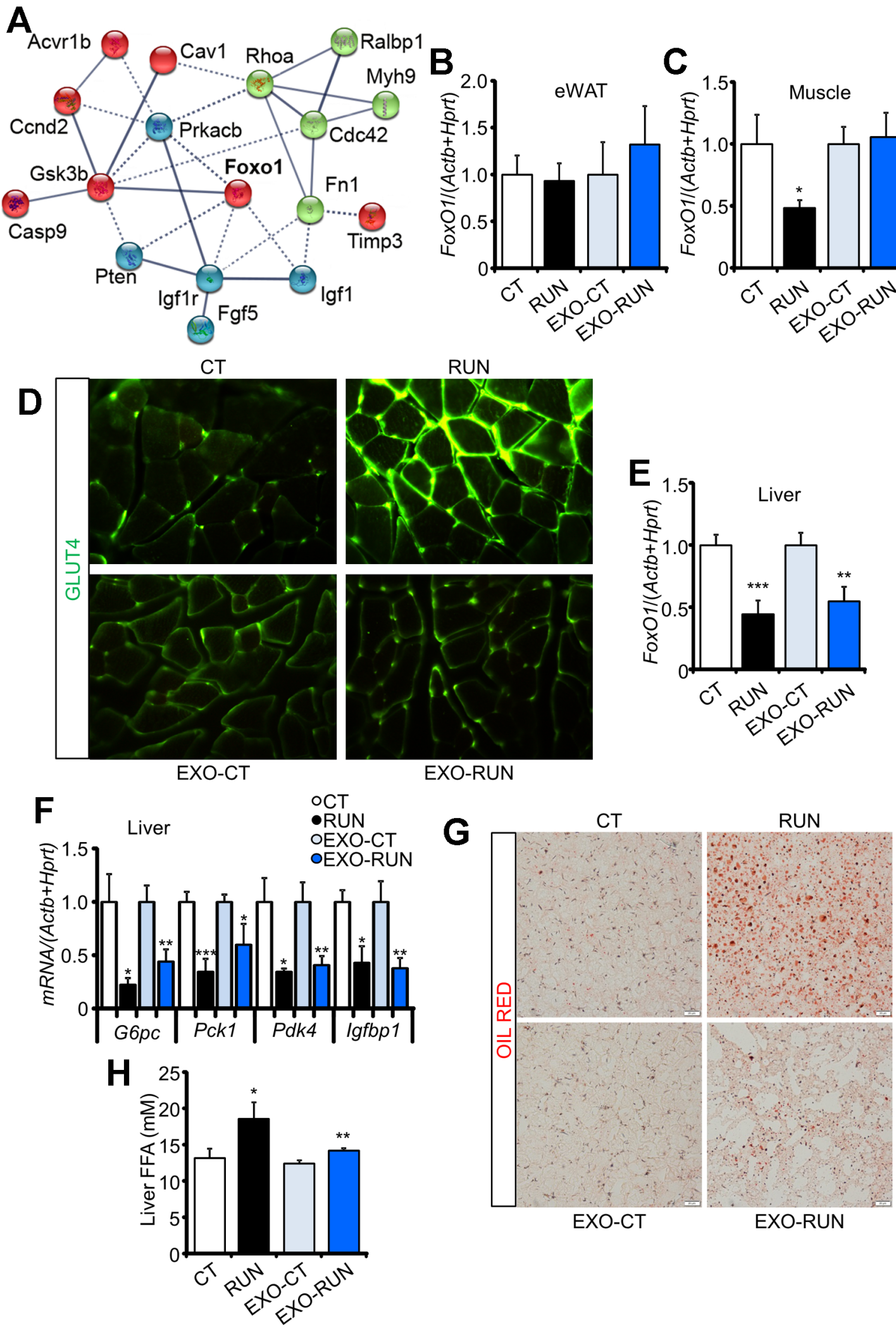
A
Acvr1b
Cav1
Rhoa
Ralbp1
Myh9
Ccnd2
Prkacb
Cdc42
Gsk3b
Foxo1
Fn1
Casp9
Timp3
Pten
Igf1r
Igf1
Fgf5
B
eWAT
FoxO1/(Actb+Hprt)
CT
RUN
EXO-CT
EXO-RUN
C
Muscle
FoxO1/(Actb+Hprt)
CT
RUN
EXO-CT
EXO-RUN
D
CT
RUN
GLUT4
EXO-CT
EXO-RUN
E
Liver
FoxO1/(Actb+Hprt)
CT
RUN
EXO-CT
EXO-RUN
F
Liver
CT
RUN
EXO-CT
EXO-RUN
mRNA/(Actb+Hprt)
G6pc
Pck1
Pdk4
Igfbp1
G
CT
RUN
OIL RED
EXO-CT
EXO-RUN
H
Liver FFA (mM)
CT
RUN
EXO-CT
EXO-RUN

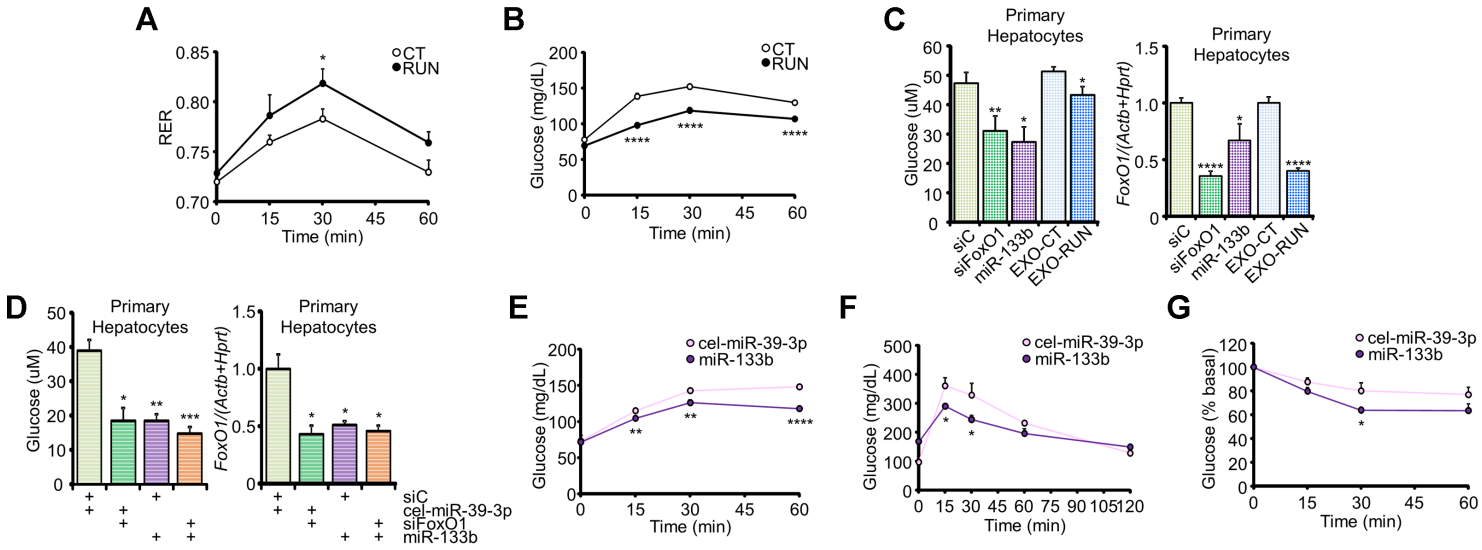
A
RER
Time (min)
CT
RUN
B
Glucose (mg/dL)
Time (min)
CT
RUN
C
Primary Hepatocytes
Glucose (uM)
FoxO1/(Actb+Hprt)
siC
siFoxO1
miR-133b
EXO-CT
EXO-RUN
D
Primary Hepatocytes
Glucose (uM)
FoxO1/(Actb+Hprt)
siC
cel-miR-39-3p
siFoxO1
miR-133b
E
Glucose (mg/dL)
Time (min)
cel-miR-39-3p
miR-133b
F
Glucose (mg/dL)
Time (min)
cel-miR-39-3p
miR-133b
G
Glucose (% basal)
Time (min)
cel-miR-39-3p
miR-133b

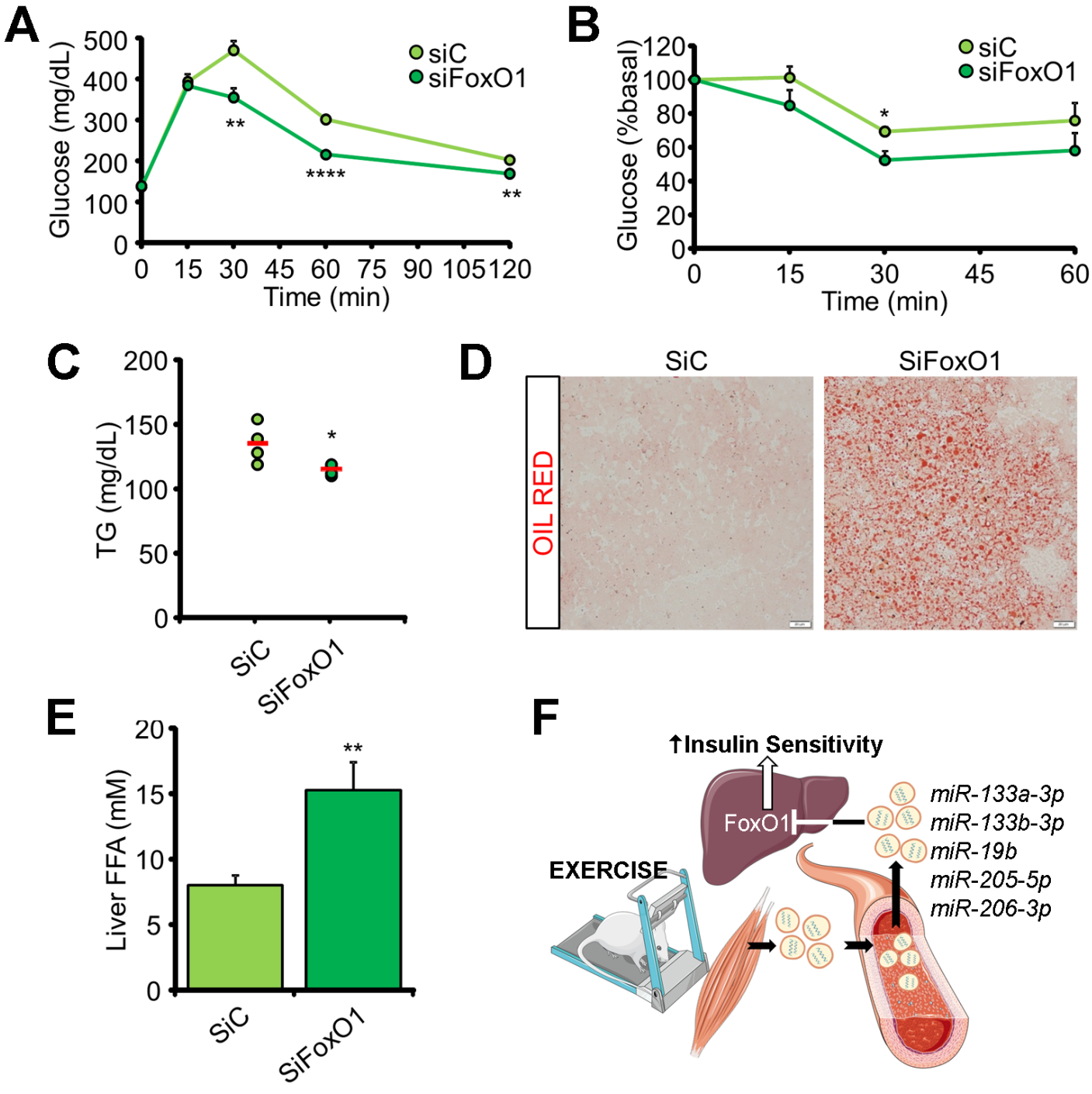
A
Glucose (mg/dL)
500
400
300
200
100
0
0 15 30 45 60 75 90 105 120
Time (min)
siC
siFoxO1
**
****
**
B
Glucose (%basal)
120
100
80
60
40
20
0
0 15 30 45 60
Time (min)
siC
siFoxO1
*
C
TG (mg/dL)
200
150
100
50
0
SiC
SiFoxO1
*
D
SiC
SiFoxO1
OIL RED
E
Liver FFA (mM)
20
15
10
5
0
SiC
SiFoxO1
**
F
↑Insulin Sensitivity
FoxO1
EXERCISE
miR-133a-3p
miR-133b-3p
miR-19b
miR-205-5p
miR-206-3p